Proceedings of the ASME 2011 Pressure Vessels & Piping Conference
PVP2011
July 17-21, 2011, Baltimore, Maryland, USA

PVP2011-57162

TIME-DOMAIN MODELING OF THE RANDOM VIBRATIONS OF TUBES SUBJECTED TO TURBULENCE-CONVEYING FLOWS

Jose Antunes
Instituto Tecnologico e Nuclear
Applied Dynamics Laboratory
ITN, ADL
Sacavem, Portugal

Xavier Delaune
Commissariat à l'Energie Atomique et aux Energies Alternatives
Laboratoire d'Études de Dynamique
CEA, DEN, DM2S, SEMT, DYN
Saclay, France

Philippe Piteau
Commissariat à l'Energie Atomique
et aux Energies Alternatives
Laboratoire d'Études de Dynamique
CEA, DEN, DM2S, SEMT, DYN
Saclay, France

ABSTRACT

The vibrations of multi-supported tubes subjected to flow excitation have been the subject of active research for many years, in particular connected with the critical design of heat exchangers and fuel bundles of nuclear power facilities. Because tubes are often loosely supported, their nonlinear dynamics are conveniently addressed through time-domain numerical simulations. Turbulence is one of the main excitation mechanisms which drive tube vibrations. Recently, we revisited the problem of random excitation generation in the time domain, by properly emulating the spectral and spatial features of the turbulence force field due to transverse flows. A new simplified an efficient technique was developed, which we successfully compared with a generation method based on the classical work by Shinozuka.

In the present paper, we pursue such work by modeling flows which display a significant axial velocity component, leading to the convection of turbulence fluctuations. This problem has been addressed by many authors in the past, mainly focusing on the frequency-based vibratory analysis of flow-excited plates, pipes and tubes. Here, we focus on several techniques for generating time-domain turbulence excitations which properly account for the axial turbulence transport term of convective flows. More specifically, we start by applying two random force generation methods to emulate axial turbulent flows and evaluate the practical significance of the cross-spectral convection delay term. We discuss the use of forces applied at fixed locations, the use of travelling forces being also investigated. Finally, we discuss the correlation of random forces along two orthogonal directions, when simulating two-dimensional turbulence fields.

NOMENCLATURE

C_p	Amplitude coefficients of the uncorrelated random forces which simulate turbulence
D	Tube diameter
f	Frequency
f_n	Modal frequencies
f_R	Reduced frequency
$F_s(t)$	Contact/friction force at support x_s
$F_n(t)$	Modal force
$f_A(x,t)$	Distributed force field from the axial turbulence
$f_T(x,t)$	Distributed force field from the transverse turbulence
$\{f_p(t)\}$	Set of random point forces which simulates the continuous turbulence force field
$H_n(\omega)$	Modal complex amplitude response of the system transfer functions
k	Index of the spectra frequencies

K	Number of positive and negative frequencies where spectral components are defined
l	Index of the POD eigenvalues/eigenvectors
L	Tube length; number of POD components
$L_{An}(f)$	Joint-acceptance correlation integral for axial turbulence (mode n)
$L_{Tn}(f)$	Joint-acceptance correlation integral for transverse turbulence (mode n)
m_n	Modal mass
$[M(f)]$	Frequency dependent signal mixing matrix
$n = 1, 2, ..., N$	Modal index
N_t	Number of time samples
P	Number of random point forces used to simulate the turbulence excitation
$q_n(t)$	Modal response
$\{r_s(t)\}$	Statistically independent random functions
$\{R_s(f)\}$	Fourier transform of the statistically independent random functions
$S_{pp}(x_i, x_j, f)$	Cross-spectra between correlated point forces
$S_A(x_1, x_2, \omega)$	Cross-spectrum of the axial turbulence $f_A(x,t)$
$S_T(x_1, x_2, \omega)$	Cross-spectrum of the transverse turbulence $f_T(x,t)$
$[S_{pp}(f)]$	Cross-spectrum matrix of the correlated point forces
$S_{q_n q_n}(\omega)$	Auto-spectrum of the modal response $q_n(t)$
$S_{q_n q_m}(\omega)$	Cross-spectrum of the modal responses $q_n(t)$ and $q_m(t)$
$S_{yy}(x, \omega)$	Auto-spectra of the response $Y(x,t)$
$S_{zz}(x, \omega)$	Auto-spectra of the response $Z(x,t)$
t	Time
V_C	Convection velocity of the turbulence eddies in axial flows
V_A	Flow axial velocity (assumed constant)
V_T	Flow transverse velocity (assumed constant)
x	Axial location along the tube
x_p	Axial location of the random point forces which simulate the turbulence excitations
y, z	Orthogonal motion directions
$Y(x,t), Z(x,t)$	Flexural responses
δ^*	Displacement thickness of the boundary layer
Δf	Step between discretized spectral frequencies
Δx_p	Distance between two neighbor point forces used to simulate the turbulence excitation
$\gamma_A(x_1, x_2, \omega)$	Space coherence function of the turbulence excitation from an axial flow
$\gamma_T(x_1, x_2, \omega)$	Space coherence function of the turbulence excitation from a transverse flow
$\gamma_{ij}(f)$	Coherence functions between the correlated point forces
$\lambda_l(f), \{\psi_l(f)\}$	Eigenvalues and eigenvectors from the POD decomposition of $[S_{pp}(f)]$
$[\Lambda(f)], [\Psi(f)]$	Matrices of the eigenvalues and eigenvectors from the POD decomposition of $[S_{pp}(f)]$
$\lambda_A(\omega)$	Axial correlation length of the turbulence excitation from an axial flow
$\lambda_T(\omega)$	Axial correlation length of the turbulence excitation from a transverse flow
φ_k	Random spectral phase angle
$\Phi_P(\omega)$	Local auto-spectrum of the pressure field
$\overline{\Phi}(f_R)$	Dimensionless spectrum of the local turbulence excitation
$\Phi_A(x, \omega)$	Local auto-spectrum of the turbulence excitation from an axial flow
$\Phi_T(x, \omega)$	Local auto-spectrum of the turbulence excitation from a transverse flow
$\Phi_{exc}(f)$	Auto-spectrum of the uncorrelated point forces which simulate turbulence
$\Phi_p(x_p, f)$	Auto-spectrum of the uncorrelated point forces which simulate turbulence
$\chi_{yy}(\lambda_\theta)$	Azimuthal coefficient for the auto-spectrum of the random force $F_A^y(t)$
$\chi_{zz}(\lambda_\theta)$	Azimuthal coefficient for the auto-spectrum of the random force $F_A^z(t)$
$\chi_{yz}(\lambda_\theta)$	Azimuthal coefficient for the cross-spectra of the random forces $F_A^y(t)$ and $F_A^z(t)$
ρ	Flow density (assumed constant)
ω	Circular frequency
ω_n	Modal circular frequency
ζ_n	Modal damping
$\varphi_n(x)$	Mode shape
σ_k	Spectral amplitude coefficients

INTRODUCTION

Predictive computations of the dynamical responses of multi-supported tubes subjected to flow excitation have been the subject of active research for many years, in particular connected with the critical design of heat exchangers and fuel bundles of nuclear power facilities. The need to assert the suitability and expected life of these components triggered the development of computational methods for predictive vibratory analysis under realistic conditions. Because tubes are often loosely supported, their nonlinear dynamics are conveniently addressed through time-domain numerical simulations.

Turbulence is one of the main excitation mechanisms which drive tube vibrations and a component life controlling factor, in the long range. Recently, we revisited the problem of random excitation generation, in order to properly emulate the spectral and spatial features of the turbulence force field due to transverse flows, see Axisa et al. [1] for a general overview of the problem. A new simplified an efficient technique for generating random force fields with suitable spectral and space correlation properties was developed, see Antunes et al. [2], which we later successfully compared with a more involved POD (Proper Orthogonal Decomposition) force generation method [3] based on the classical work by Shinozuka et al. [4]. In the present paper, we pursue our previous work by addressing the time-domain generation of turbulent force fields stemming from flows which display a significant axial velocity component.

The phenomenological characterization of the turbulence excitation by axial flows has been addressed by many authors in the past, since the pioneering work of Corcos [5], Clinch [6], Willmarth & Wooldridge [7], Bull [8], Bakewell [9] and Gorman [10], among others, but also in more recent times, see Au-Yang [11]. These authors mainly focused on the frequency domain vibratory analysis of flow-excited plates, pipes and tubes, through the corresponding correlation integrals, the so-called joint and cross-acceptances. Although the main bulk of their findings is well established, important points are still open to debate, such as the behavior of the turbulence correlation lengths as a function of frequency and of the flow velocity, see for instance Durant et al. [12] and Leclercq & Bohineust [13].

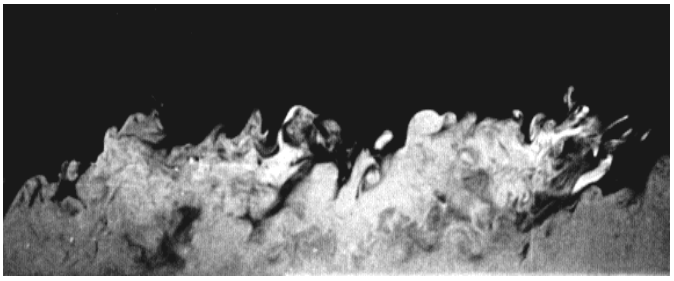

Figure 1: Boundary layer turbulence generated by axial flow on a wall at $\mathrm{Re} = 4000$ **based on the momentum thickness [14]**

As illustrated in Figure 1, borrowed from [14], the boundary layer turbulence structures generated by axial flows are quite distinct from those displayed by the turbulence of separated transverse flows. In particular, the turbulence generation mechanism in axial flows is intrinsically connected with the convection of the turbulence fluctuations. Therefore, although the formulations used to model the fluctuations cross-spectra from transverse and axial flows present a number of similarities, it is important to keep in mind that the physical phenomena involved are quite distinct.

Here, we focus on several techniques for extending our previous work in order to deal with convective flows. More specifically, we start by applying the force generation methods [2,3] to axial turbulent flows and evaluate the practical significance of the cross-spectral convection delay term. Then, focusing on our implementation of Shinozuka's technique [3], which generates a set of partially correlated random forces, we discuss the use of excitations applied at fixed locations along the tube, as well as the use of forces travelling at the convection velocity, for emulating different types of turbulence excitation. Finally, we provide some comments on two-dimensional force fields, concerning the possible correlation of the random excitations along the two orthogonal directions.

EXCITATION FROM TRANSVERSE FLOWS

We start by recalling well known results concerning the linear vibratory responses of tubes subjected to the turbulence excitation of cross-flows. Consider a tubular structure with length L, external diameter D and modal properties m_n, ω_n, ζ_n and $\phi_n(x)$, which for the sake of simplicity will be assumed identical for the two orthogonal mode sets related to the y and z motions. The tube is subjected to random force fields $f_T^y(x,t)$ and $f_T^z(x,t)$ due to the turbulence excitation from a transverse flow described by its density $\rho(x)$ and transverse velocity $V_T(x)$ profiles along the tube. For compactness of this presentation, both profiles will be assumed uniform, $\rho(x) \equiv \rho$ and $V_T(x) \equiv V_T$, $\forall x$, however full details on the general formulation for non-uniform flows are provided in the papers by Axisa et al. [1] and Antunes et al. [2].

The linear tube responses are formulated in terms of the modal equations $(n = 1, 2, ..., N)$:

$$m_n \ddot{q}_n^y + 2 m_n \omega_n \zeta_n \dot{q}_n^y + m_n \omega_n^2 q_n^y = F_n^y(t) \qquad (1)$$

$$m_n \ddot{q}_n^z + 2 m_n \omega_n \zeta_n \dot{q}_n^z + m_n \omega_n^2 q_n^z = F_n^z(t) \qquad (2)$$

with the physical responses $Y(x,t)$ and modal forces $F_n^y(t)$ computed as:

$$Y(x,t) = \sum_{n=1}^{N} \phi_n(x)\, q_n^y(t) \quad ; \quad F_n^y(t) = \int_0^L \phi_n(x)\, f_T^y(x,t)\, dx \qquad (3)$$

and similarly for the orthogonal motion and modal forces:

$$Z(x,t)=\sum_{n=1}^{N}\phi_n(x)\,q_n^z(t) \quad ; \quad F_n^z(t)=\int_0^L \phi_n(x)\,f_T^z(x,t)\,dx \quad (4)$$

The dynamics along both directions are dealt similarly, therefore we will drop in the following the superscripts y,z. In actual nonlinear tube analysis, when computing the modal forces $F_n(t)$, the turbulence force terms in equations (3) and (4) will be supplemented by contact/friction forces $F_s(t)$ at the $s=1,2,...,S$ clearance supports, see [1]:

$$F_n(t)=\int_0^L \phi_n(x)\,f_T(x,t)\,dx+\sum_{s=1}^{S}\phi_n(x_s)F_s(t) \quad (5)$$

and other flow terms may be included in (5) if the fluid-elastic forces are accounted for, as thoroughly discussed by Piteau et al. [15]. However, such aspects are out of the scope of the present paper.

Then, from well established results in the theory of random vibrations, the cross-spectra of the modal responses are obtained as $(m=1,2,...,N\,;\,n=1,2,...,N)$:

$$S_{q_nq_m}(\omega)=H_n(\omega)H_m^*(\omega)\int_0^L\int_0^L \phi_n(x_1)\,\phi_m(x_2)\,S_T\left(x_1,x_2,\omega\right)dx_1dx_2 \quad (6)$$

where $H_n(\omega)=\left[m_n\left(\omega_n^2-\omega^2+2i\omega\omega_n\zeta_n\right)\right]^{-1}$ and the excitation field $f_T(x,t)$ is entirely described in terms of its cross-spectrum $S_T\left(x_1,x_2,\omega\right)$. The tube response is given by:

$$S_{yy}(x,\omega)=\sum_{n=1}^{N}\sum_{m=1}^{N}\phi_n(x)\,\phi_m(x)\,S_{q_nq_m}(\omega) \quad (7)$$

Often cross-terms are much smaller than the diagonal terms in (7), which then simplifies to:

$$S_{yy}(x,\omega)\approx\sum_{n=1}^{N}\left[\phi_n(x)\right]^2 S_{q_nq_n}(\omega) \quad (8)$$

where:

$$S_{q_nq_n}(\omega)=\left|H_n(\omega)\right|^2\int_0^L\int_0^L \phi_n(x_1)\,\phi_n(x_2)\,S_T\left(x_1,x_2,\omega\right)dx_1dx_2 \quad (9)$$

The excitation $S_T\left(x_1,x_2,\omega\right)$ from the transverse flow turbulence may be conveniently modeled in terms of a local auto-spectrum $\Phi_T\left(x,\omega\right)$ and a spatial correlation function $\gamma_T\left(x_1,x_2,\omega\right)$. For uniform flows we have $\Phi_T\left(x,\omega\right)\equiv\Phi_T\left(\omega\right)$, $\forall x$:

$$\begin{aligned}S_T\left(x_1,x_2,\omega\right)&=\left[\Phi_T(x_1,\omega)\,\Phi_T(x_2,\omega)\right]^{1/2}\gamma_T\left(x_1,x_2,\omega\right)\\&=\Phi_T(\omega)\,\gamma_T\left(x_1,x_2,\omega\right)\end{aligned} \quad (10)$$

where, for *cross-flow excitations*, the coherence function $\left|\gamma_T\left(x_1,x_2,\omega\right)\right|\le 1$ which describes the spatial correlation of the turbulence eddies is real and may, for homogeneous flows, be described using the simple form [1]:

$$\gamma_T\left(x_1,x_2,\omega\right)=\exp\left(-\frac{\left|x_2-x_1\right|}{\lambda_T(\omega)}\right) \quad (11)$$

where $\lambda_T(\omega)$ is the correlation length of transverse flow turbulence fluctuations, which for tube bundles is of the order of the tube diameter, see Inada et al. [16].

For obvious reasons it is convenient to express the turbulence spectra in dimensionless form. For single-phase flows, collapsing of experimental data is achieved by scaling Φ_T in terms of the flow pressure head and using the reduced frequency $f_R=fD/V_T$, so that the following dimensionless spectrum $\overline{\Phi}_T$ is obtained:

$$\overline{\Phi}_T(f_R)=\left(\frac{1}{2}\rho V_T^2 D\right)^{-2}\frac{V_T}{D}\Phi_T(f) \quad ; \quad f_R=\frac{fD}{V_T} \quad (12)$$

and using (9) to (12), the modal tube responses are obtained:

$$\begin{aligned}S_{q_nq_n}(f)&=\Phi_T\left(f\right)\left|H_n(f)\right|^2 L_{Tn}^2\\&=\left(\frac{1}{2}\rho V_T^2 D\right)^2\frac{D}{V_T}\overline{\Phi}_T\left(f_R\right)\left|H_n(f)\right|^2 L_{Tn}^2(f)\end{aligned} \quad (13)$$

where $L_{Tn}^2(f)$ is the so-called joint-acceptance integral, which encapsulates the combined effects of the spatial correlation of the fluctuations λ_T and the structural mode shapes $\phi_n(x)$. This is the particular case when $m=n$ of the general cross-acceptance integrals:

$$L_{Tmn}^2(f)=\int_0^L\int_0^L \phi_m(x_1)\,\phi_n(x_2)\exp\left(-\frac{\left|x_2-x_1\right|}{\lambda_T(f)}\right)dx_1dx_2 \quad (14)$$

where in general $\lambda_T(f)/L\ll 1$, which allows for interesting simplifications in (14), as discussed by Axisa et al. [1].

Following the information supplied, we now present the simple method introduced by Antunes et al. [2] to simulate the time-domain turbulence random field, which uses a set of uncorrelated random forces, as well as a general technique which generates a set of partially correlated random forces, following Shinozuka et al. [3,4].

Generation method using uncorrelated point forces

This approach uses *uncorrelated* point forces located along the tube, which are generated with spectral properties and amplitudes such that they induce the same linear modal responses as the original continuous formulation expressed by (13). For a set of P random uncorrelated point forces spaced along the tube, $\left\{f_p(t)\right\}\equiv f(x_p,t)$ with $p=1,2,...,P$, the resulting modal responses read:

$$S_{q_nq_n}(f)=\left|H_n(f)\right|^2\sum_{p=1}^{P}\left|\phi_n(x_p)\right|^2\Phi_p\left(x_p,f\right) \quad (15)$$

where $\Phi_p\left(x_p, f\right)$ is the auto-spectrum of the point force to be applied at location x_p.

We now enforce the condition that modal responses (13) and (15) be the same for all modes of interest $n = 1, 2, ..., N$:

$$\sum_{p=1}^{P} \left|\phi_n(x_p)\right|^2 \Phi_p\left(x_p, f\right) = \left(\frac{1}{2}\rho V_T^2 D\right)^2 \frac{D}{V_T} \bar{\Phi}_T\left(\frac{fD}{V_T}\right) L_{Tn}^2(f) \quad (16)$$

Based on the previous simplifying assumptions, we postulate the same spectral content $\Phi_{exc}\left(f\right)$ for each one of the equivalent point forces, so that we may write for $p = 1, ..., P$:

$$\Phi_p\left(x_p, f\right) = C_p\, \Phi_{exc}\left(f\right) \quad (17)$$

where $C_p > 0$ are unknown amplitude coefficients to be computed. Then, replacing (17) into (16), we obtain for $n = 1, 2, ..., N$:

$$\Phi_{exc}\left(f\right) \sum_{p=1}^{P} C_p \left|\phi_n(x_p)\right|^2 = \left(\frac{1}{2}\rho V_T^2 D\right)^2 \frac{D}{V_T} \bar{\Phi}_T\left(\frac{fD}{V_T}\right) L_{Tn}^2(f) \quad (18)$$

Identification of the frequency-dependent terms in (18), when the joint-acceptance integrals are computed using the correlation length values at the corresponding modal frequencies, $\lambda_T(f_n)$, leads to the excitation spectrum:

$$\Phi_{exc}\left(f\right) = \left(\frac{1}{2}\rho V_T^2 D\right)^2 \frac{D}{V_T} \bar{\Phi}_T\left(\frac{fD}{V_T}\right) \quad (19)$$

and the coefficients C_p must fulfill the following N conditions:

$$\sum_{p=1}^{P} C_p \left|\phi_n(x_p)\right|^2 = L_{Tn}^2(f_n) \quad ; \quad n = 1, 2, ..., N \quad (20)$$

whence the corresponding solution:

$$\begin{Bmatrix} C_1 \\ C_2 \\ \vdots \\ C_p \end{Bmatrix} = \begin{bmatrix} |\phi_1(x_1)|^2 & |\phi_1(x_2)|^2 & \cdots & |\phi_1(x_P)|^2 \\ |\phi_2(x_p)|^2 & |\phi_2(x_2)|^2 & \cdots & |\phi_2(x_P)|^2 \\ \vdots & \vdots & \ddots & \vdots \\ |\phi_N(x_p)|^2 & |\phi_N(x_2)|^2 & \cdots & |\phi_N(x_P)|^2 \end{bmatrix}^{+} \begin{Bmatrix} L_{T1}^2(f_1) \\ L_{T2}^2(f_2) \\ \vdots \\ L_{TN}^2(f_N) \end{Bmatrix} \quad (21)$$

which is of the least-squares type, where $\{M\}^+$ is the SVD regularized Moore-Penrose pseudo-inverse of $\{M\}$. Once the parameters of the equivalent force set (17) have been obtained, each one of the statistically independent gaussian time-domain realizations $\{f_p(t)\}$, at the P point forces, is generated using the standard Inverse Fourier Transform procedure:

$$f_p(t) = \frac{N_t}{\sqrt{2}} FFT^{-1}\left(\sigma_k\, e^{-i\varphi_k}\; ; k = -K, ..., K\right) \quad (22)$$

using, for each force location $p = 1, 2, ..., P$, sampled random phases uniformly distributed in the range $\varphi_k \in [0 \;\; 2\pi]$ and the spectral amplitudes:

$$\sigma_k = \sqrt{\Phi_{exc}(f_k)\,\Delta f} \quad (23)$$

A generalization of this procedure can be applied to non-uniform flows, as explained in [2]. Typically, the procedure converges to satisfactory results whenever the number of point forces is higher than the number of modes excited.

Generation method using correlated point forces

The starting point of all spectral-based methods for generating a set of P *partially correlated* point-forces $\{f_P(t)\}$ is the frequency-dependent excitation cross-spectrum (10). In matrix terms, let us write:

$$S_{pp}\left(x_i, x_j, f\right) \equiv S_{ij}(f) = \Delta x^2 \left[\Phi_i(f)\Phi_j(f)\right]^{1/2} \gamma_{ij}\left(f\right) \;,\; i, j = 1, 2, ...P \quad (24)$$

or:

$$\left[S_{pp}(f)\right] = \begin{bmatrix} S_{11}(f) & S_{12}(f) & \cdots & S_{1P}(f) \\ S_{21}(f) & S_{22}(f) & \cdots & S_{2P}(f) \\ \vdots & \vdots & \ddots & \vdots \\ S_{P1}(f) & S_{P2}(f) & \cdots & S_{PP}(f) \end{bmatrix} \quad (25)$$

where $\Delta x = L/P$ is the flow-subjected tube region connected with each point force, within which the turbulence excitation is tacitly assumed correlated. For obvious reasons, one should expect that $\Delta x < \lambda_T(f)$ within the frequency range of interest, for an adequate simulation of the random field.

Among the techniques developed following Shinozuka's original Cholesky decomposition of $\left[S_{pp}(f)\right]$, we exploit here the elegant approach based on the Proper Orthogonal Decomposition (POD) of (24), also known as Karhunen-Loeve expansion. We wish to create partially correlated random signals $\{f_p(t)\}$ such that their Fourier transform $\{F_p(f)\}$ cope with (24). These signals are generated by mixing statistically independent signals $\{r_s(t)\}$, with Fourier transforms $\{R_s(f)\}$, so that :

$$\{F_p(f)\} = [M(f)]\{R_s(f)\} \quad (26)$$

where $[M(f)]$ are frequency dependent mixing matrices. Then, from (26), we obtain:

$$\{F_p(f)\}\{F_p(f)\}^H = [M(f)]\{R_s(f)\}\{R_s(f)\}^H [M(f)]^H \quad (27)$$
$$\Rightarrow \quad \left[S_{pp}(f)\right] = [M(f)][S_{ss}(f)][M(f)]^H$$

On the other hand, for each frequency f one may perform an eigen-decomposition of $\left[S_{pp}(f)\right]$:

$$\left[S_{pp}(f)\right][\Psi(f)] = [\Lambda(f)][\Psi(f)] \text{ with } [\Psi(f)]^H[\Psi(f)] = [I] \quad (28)$$

where matrix $[\Lambda(f)] = Diag\left[\lambda_1(f), \lambda_2(f), ..., \lambda_L(f)\right]$ contains the $L = P$ eigenvalues of $\left[S_{pp}(f)\right]$, while the columns of $[\Psi(f)] \equiv [\{\psi_1(f)\}, \{\psi_2(f)\}, ..., \{\psi_L(f)\}]$ contain the corresponding eigenvectors. Because matrices $\left[S_{pp}(f)\right]$ are Hermitian positive-definite, their eigenvalues $\lambda_l(f)$ are always real and

positive, while the eigenvectors $\{\psi_l(f)\}$ are in general complex. From (28) one can state the following relations:

$$\begin{aligned} &[\Psi(f)]^H [S_{pp}(f)][\Psi(f)] = [\Lambda(f)] \\ \Rightarrow \quad &[S_{pp}(f)] = [\Psi(f)][\Lambda(f)][\Psi(f)]^H \end{aligned} \tag{29}$$

If we now build the mixing matrices $[M(f)]$ in (26) using the eigenvectors of $[S_{pp}(f)]$, we have:

$$[M(f)] \equiv [\Psi(f)] \quad \Rightarrow \quad \{F_p(f)\} = [\Psi(f)]\{R_s(f)\} \tag{30}$$

or, from (29) and (30):

$$\begin{aligned} &[S_{pp}(f)] = [\Psi(f)][S_{ss}(f)][\Psi(f)]^H \\ \Rightarrow \quad &[S_{ss}(f)] = \{R_s(f)\}\{R_s(f)\}^H = [\Lambda(f)] \end{aligned} \tag{31}$$

Hence, $[\Lambda(f)]$ stands as cross-correlation matrices of the statistically independent signals $\{R_s(f)\}$, and are thus naturally diagonal. The preceding formulation supplies a convenient method for the generation of the partially correlated random forces $\{f_p(t)\}$. Using the Inverse Fourier Transform technique (with the number of time and frequency samples related as $N = 2K+1$), the correlated forces arise as the sum of L independent principal component (POD) force terms:

$$\begin{aligned} \{f_p(t)\} &= \sum_{l=1}^{L} \{f_p^l(t)\} \\ &= \frac{N_t}{\sqrt{2}} \sum_{l=1}^{L} FFT^{-1}\left(\{\sigma_{pk}^l\} e^{-i\varphi_k^l} \; ; k = -K, ..., K\right) \end{aligned} \tag{32}$$

with, for each force location $p = 1, 2, ..., P$ and each component $l = 1, 2, ..., L$, the spectral amplitudes:

$$\{\sigma_{pk}^l\} = \{\psi_l(f_k)\}\left\{\sqrt{\lambda_l(f_k)\,\Delta f}\right\} \tag{33}$$

and using sampled random phases uniformly distributed in the range $\varphi_k^l \in [0 \; 2\pi]$, for each orthogonal component $l = 1, 2, ..., L$. Partial correlation of the forces $\{f_p(t)\}$ then stems from the superposition of the L terms $\{f_p^l(t)\}$. When all principal components are used, the number of independent signals generated equals the number of correlated point forces, $L = P$.

This general procedure for generating a random force field is more versatile than the simplified method previously described. However, it asks for much higher computer resources, so that the time-domain excitation generation often becomes as computer intensive as the nonlinear numerical simulation which follows.

EXCITATION FROM AXIAL FLOWS

Generalization of the previous techniques to deal with turbulent *axial flows excitations* is quite straightforward. The main difference stems from the cross-spectrum of axial flow turbulence, which now includes a convection term:

$$S_A(x_1, x_2, \omega) = \Phi_A(\omega)\, \gamma_A(x_1, x_2, \omega) \tag{34}$$

where the spatial correlation function $\gamma_A(x_1, x_2, \omega)$ is formulated following the phenomenological model attributed to Corcos [5] for the cross-correlation of the pressure field at the wall surface, whose main features have been firmly established through a large number of experiments, see [6-10]. With respect to a fixed reference frame, the complex coherence in (34) reads:

$$\gamma_A(x_1, x_2, \omega) = \exp\left(-\frac{|x_2 - x_1|}{\lambda_A(\omega)}\right) \exp\left(i \frac{x_2 - x_1}{V_C(\omega)/\omega}\right) \tag{35}$$

where $\lambda_A(\omega)$ is a correlation length of the axial flow turbulence fluctuations, while $V_C(\omega)$ is the downstream convection velocity of the turbulence eddies. The second term of (35) points to the phase difference between the excitations at x_1 and x_2, which corresponds to a time delay $\tau(\omega) = (x_2 - x_1)/V_C(\omega)$. This phase term represents the typical excitation from a rough road with random surface, as "seen" by a vehicle with relative velocity $V_C(\omega)$, see Figure 2. This is the limit case for which Taylor's "frozen turbulence" hypothesis $\partial p/\partial t = -\partial p/\partial x$ strictly applies. However, turbulence structures (e.g. the road profile) statistically change more or less as the flow progresses, as governed by the correlation length $\lambda_A(\omega)$ in the decreasing exponential term of (35). Notice that this form of turbulence is physically non dissociable from the axial flow velocity and therefore simply cannot exist if $V_A = 0$. It would be wrong to see formulation (35) as representing a kind of transverse flow turbulence (11) axially convected at velocity V_C, which is a different thing. And, indeed, when replacing $V_C \to 0$ in formulation (35), we certainly do not obtain (11).

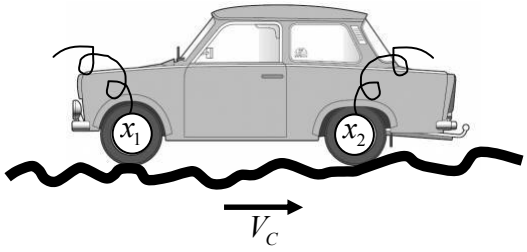

Figure 2: Analogy between Taylor's frozen turbulence and a travelling vehicle on a rough road

A large body of work has been produced for quantifying the various parameters in formulation (34)-(35), for internal pipe flows [5,6] or external flows over plates [7,8] and cylinders [9,10]. Typically, the frequency dependent axial correlation length is given by [17]:

$$\lambda_A(\omega) = V_C(\omega)/(\alpha\omega) \quad \text{with} \quad \alpha \approx 0.1 \tag{36}$$

which closely follows the results [6-8], while the convection velocity is expressed through the empirical relation, in agreement with [9]:

$$V_C(\omega) = V_A\left[0.6 + 0.4\exp\left(-2.2\omega\delta^*/V_A\right)\right] \qquad (37)$$

where δ^* is the displacement thickness of the boundary layer, see [11] for details.

Corcos model has been criticized for unrealistic behavior at low frequencies, in particular leading to unity coherence everywhere as $\omega \to 0$, see [13]. Bull [8] suggested that, at low frequencies, the coherence (35) becomes independent of frequency, whereas at higher frequencies it depends on the Strouhal number. He found this qualitative change to occur at about $\omega\delta^*/V_C(\omega) \approx 0.36$.

Generation method using uncorrelated point forces

Our simplified excitation generation method previously presented can be easily extended to deal with axial flow turbulence, by replacing the joint-acceptance integrals L^2_{Tn} in equation (21) with the corresponding values in axial flow, computed from the corresponding integrals (with $m = n$) obtained from the coherence function (35):

$$L^2_{Amn}(f) = \int_0^L\int_0^L \phi_m(x_1)\phi_n(x_2)\exp\left(-\frac{|x_2 - x_1|}{\lambda_A(f)}\right)\exp\left(i\frac{x_2 - x_1}{V_C(f)/(2\pi f)}\right)dx_1dx_2 \qquad (38)$$

Notice that, contrary to the real values of $L^2_{Tmn}(f)$ in (14), the cross-acceptance integrals of axial flow turbulence $L^2_{Amn}(f)$ are in general complex, with:

$$\mathrm{Re}\left[L^2_{Amn}(f)\right] = \int_0^L\int_0^L \phi_m(x_1)\phi_n(x_2)\exp\left(-\frac{|x_2 - x_1|}{\lambda_A(f)}\right)\cos\left(\frac{x_2 - x_1}{V_C(f)/(2\pi f)}\right)dx_1dx_2 \qquad (39)$$

$$\mathrm{Im}\left[L^2_{Amn}(f)\right] = \int_0^L\int_0^L \phi_m(x_1)\phi_n(x_2)\exp\left(-\frac{|x_2 - x_1|}{\lambda_A(f)}\right)\sin\left(\frac{x_2 - x_1}{V_C(f)/(2\pi f)}\right)dx_1dx_2 \qquad (40)$$

However, as shown by Bolotin [18], if one neglects cross-modal interactions and only the joint-acceptances are of interest, then sole the real part of (38) is relevant. To illustrate the practical effect of the convective term, let us compute (39) for the simple case of a pinned-pinned beam, as a function of axial correlation length and convection velocity. In dimensionless form, the joint-acceptance from (39) reads:

$$\overline{L}^2_{An}(f) = \int_0^1\int_0^1 \phi_n(\overline{x}_1)\phi_n(\overline{x}_2)\exp\left(-\frac{|\overline{x}_2 - \overline{x}_1|}{\overline{\lambda}_A(f)}\right)\cos\left(\frac{\overline{x}_2 - \overline{x}_1}{\overline{X}_C(f)}\right)d\overline{x}_1d\overline{x}_2 \qquad (41)$$

where $\overline{x} = x/L$, $\overline{\lambda}_A(f) = \lambda_A(f)/L$, $\overline{X}_C(f) = V_C(f)/(2\pi fL)$ and $\overline{L}^2_{An}(f) = L^2_{An}(f)/L^2$.

Notice that, in this formulation, the phase-lag convection term is ignored when assuming $\overline{X}_C(f) \to \infty$. The integral (41) was computed analytically for all mode shapes of the form $\phi_n(\overline{x}) = \sin(n\pi\overline{x})$, but the result is too involved to be usefully reported here. Instead, we plot in Figure 3 the values of $\overline{L}^2_{An}(f)$, for the first two modes of the beam, as a function of $\overline{\lambda}_A(f)$ and $\overline{X}_C(f)$. These plots have been computed over a very large range of values $\overline{\lambda}_A(f)$, however only those such that $\overline{\lambda}_A(f) \ll 1$ are typically of physical interest. One can notice that for the first mode, which is symmetrical, accounting for the phase convection term $\overline{X}_C(f)$ always leads to lower values of the beam vibratory amplitude. Such difference increases very significantly as the axial correlation increases and the convection velocity decreases. Results for the second mode, which is anti-symmetrical, are less obvious. However, in the lower range $\overline{\lambda}_A(f) \ll 1$ of interest, the same scenario applies.

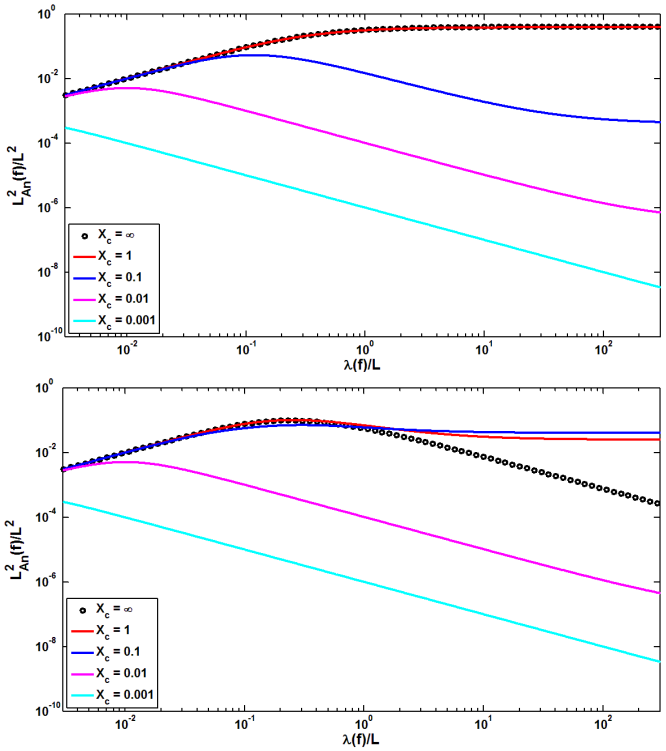

Figure 3: Normalized joint acceptances for the first two modes of a pinned-pinned beam as a function of $\overline{\lambda}_A(f)$ and $\overline{X}_C(f)$: Mode 1, upper plots; Mode 2, lower plots

One may conclude from these plots that ignoring the convection term usually overestimates the tube vibration amplitude predictions, an overestimation which can be very significant at low values of the convection velocity. A more specific representation of the global effects from the axial turbulence excitation is obtained by replacing the general parameter $\overline{\lambda}_A(\omega)$ in (41) by the axial correlation length model

(36), hence $\overline{\lambda}_A(\omega) = 10V_C(\omega)/\omega L = 10\overline{X}_C(f)$. The results then obtained are plotted in Figure 4, for the first five beam modes. The lower plots were computed including the phase convection term in equation (41), while the upper plots were computed by neglecting the convection term. These plots further highlight our previous conclusion on the serious overestimation of the predicted vibratory levels at low convection velocities, if the convection term in (41) is ignored.

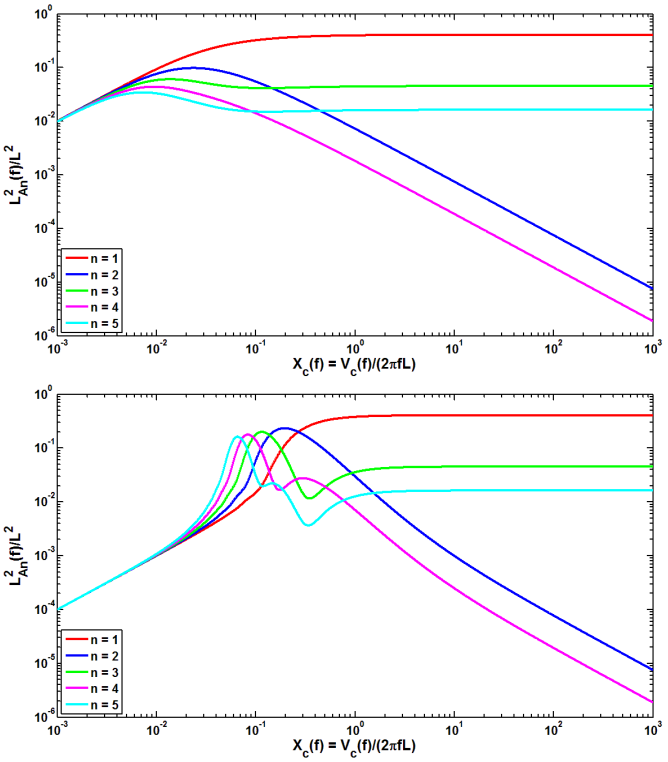

Figure 4: Normalized joint acceptances for the first five modes of a pinned-pinned beam as a function of $\overline{X}_c(f)$ for $\overline{\lambda}_A(f) = 10\overline{X}_c(f)$: Neglecting the convection term, upper plots; Including the convection term, lower plots

Time-domain numerical simulations using the proposed simplified excitation generation method are not shown here for lack of space. Nevertheless, the validation computations performed for a linear tube confirmed that this technique produces correct results and is effective for simulating the random excitation by axial turbulent flows.

Generation method using correlated point forces

The general excitation generation method described for transverse flows also applies readily to axial flows. If the complex cross-spectra (34)-(35) are used for building the spectral matrix (25) of the random point forces, then one obtains directly the time-lagged partially correlated excitations with the adequate spectral and spatial features.

If the convection velocity V_C is the same for all frequencies of interest, a more restricted but equivalent method is to generate the point forces using real cross-spectra of the form (11), e.g. "neglecting" the convection term in (35) for generating a set of provisional time-domain forces $F_p^0(t)$, which are then lagged in the following manner:

$$F_p(t) = F_p^0(t - \tau_p) \quad \text{with} \quad \tau_p = (x_p - x_0)/V_C \tag{42}$$

where x_0 is any reference location.

To illustrate the actual generation results for a set of correlated point forces using the general method, we show in Figure 6 the time-histories of five of these, which were computed from a complex cross-spectral matrix of which a few neighbor terms are shown in Figure 5 (in the form of amplitude and phase spectra, as a function of frequency). For these simulations, a tube with $L = 1$ m and $D = 0.02$ m was used, acted by a total of $P = 51$ random point forces, with $\Delta x_p = 0.02$ m. The flow excitation was assumed uniform, with an axial velocity $V_A = 5$ m/s.

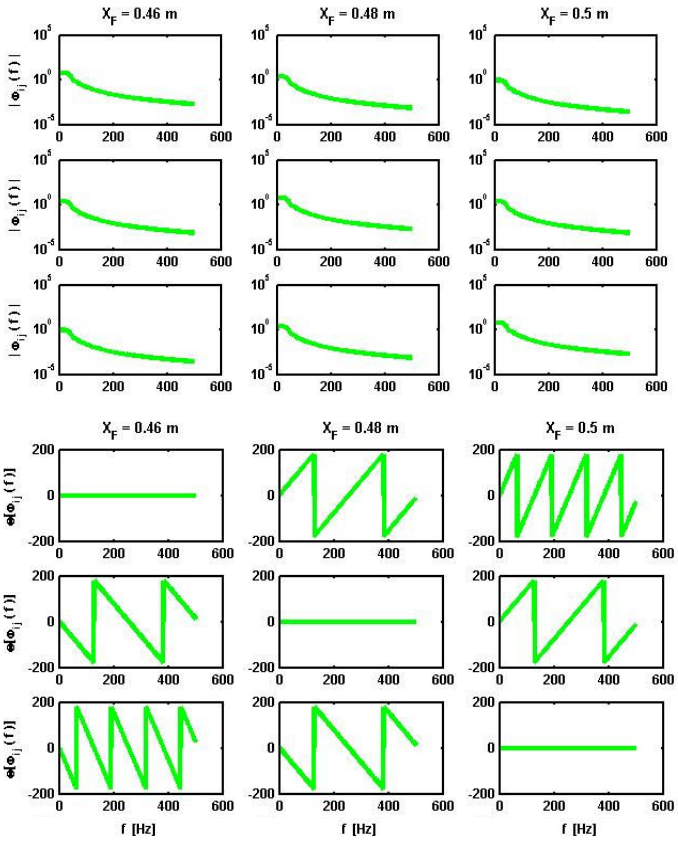

Figure 5: Some of the neighbor terms of the frequency dependent cross-spectral matrix for the point forces which simulate the turbulence excitation by an axial flow: Amplitude cross-spectra, upper plots; Phase cross-spectra, lower plots

The computations of Figures 5 and 6 were performed assuming a low value of the space correlation $\lambda_A = D = 0.02$ m and the convection velocity $V_C = V_A = 5$ m/s. On can notice the lag effects on the phase spectra shown in Figure 5. The partially correlated resulting point forces illustrated in Figure 6 also encapsulate the convection time lag, an effect which is not well perceived because of the small axial correlation length used for this computation, $\lambda_A = D = 0.02$ m, which leads to a low "memory" of the generated signals, as the turbulence convects. The signals in this example depart somewhat from the frozen turbulence scenario. On the contrary, a significant "memory" effect on the convected turbulence become evident for the simulation results shown in Figure 7 using a higher correlation length, $\lambda_A = 10D = 0.2$ m. These results clearly illustrate the convection time lags between the well correlated point forces.

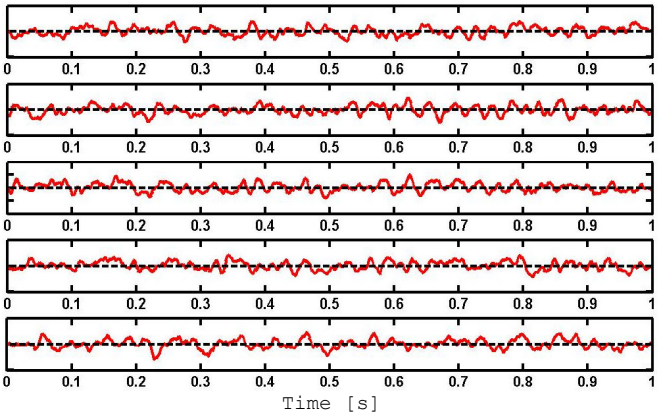

Figure 6: Samples of the generated neighbor correlated time-domain random point forces, simulated using parameters postulated frequency independent:

$\lambda_A = D = 0.02$ m **and** $V_C = V_A = 5$ m/s

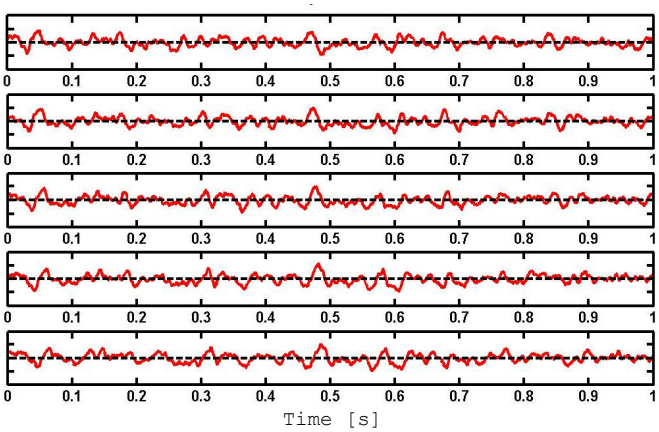

Figure 7: Samples of the generated neighbor correlated time-domain random point forces, simulated using parameters postulated frequency independent:

$\lambda_A = 10D = 0.2$ m **and** $V_C = V_A = 5$ m/s

Again, the time-domain vibratory responses computed for validation under linear conditions, using excitations generated with this general method, led to satisfactory results.

Axial convection of transverse turbulence

At this point, the reader may wonder about the dynamical effects of the turbulence excitation from a transverse flow if the corresponding random force field is also subjected to an axial transport at velocity V_C. This hypothetical case, which was mentioned before in the paper, may be seen as being purely speculative, or else considered as a real physical possibility. We will not debate here on which should be the most physically plausible manner of tackling the problem of oblique flows, but will be simply interested in using the computational tool developed to investigate this case.

Therefore, using the force generation technique based on correlated point forces, we generated a set based on the real cross-correlation (11) for transverse turbulence. These random forces were then convected axially with velocity V_C and projected on the tube modes at the corresponding mobile locations $\{x_p(t)\} = \{x_p(t_0) + V_C \Delta t\}$. Illustrative results are shown in Figure 8, which shows the root-mean-square amplitude responses of the first 3 tube modes, for a given transverse flow velocity V_T, as a function of the convection velocity V_C. These results pertain to a correlation length $\lambda_T / L = 0.1$, but a similar scenario was obtain for other values of the correlation.

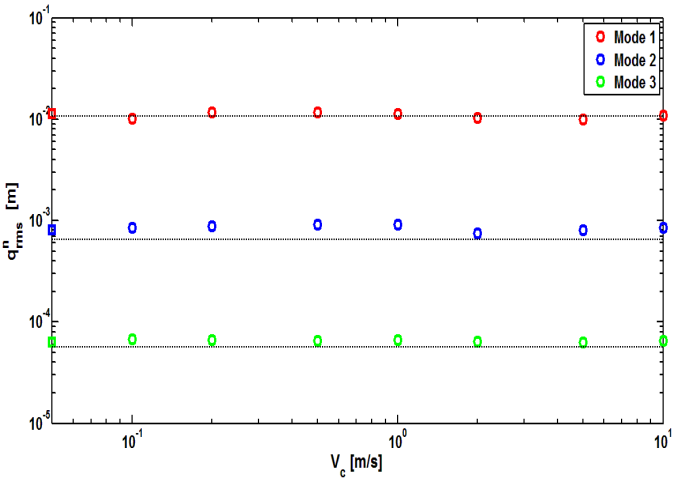

Figure 8: Vibratory responses of a tube subjected to the random excitation of a transverse flow, which is axially convected at velocity V_C

From this data it can be concluded that the vibratory responses to a transverse turbulence excitation which is axially convected are totally insensitive to the convection velocity V_C,

irrespective of the turbulence correlation length. This behavior is in clear contrast to the behavior of axial turbulence excitations, as displayed in Figure 4.

TWO-DIMENSIONAL FORCE FIELDS

An aspect often casually addressed in the literature is the correlation between the two orthogonal excitation forces $f^{y}_{A,T}(x,t)$ and $f^{z}_{A,T}(x,t)$, which result from the turbulence pressure field $p(\theta,x,t)$. Actually, most often the orthogonal forces are simply postulated uncorrelated, without any further argument. In fact, for axial flows such assumption is easily justified, from the pressure cross-spectrum:

$$S_P(\theta_1,\theta_2,x_1,x_2,\omega)=\Phi_P(\omega)\gamma(\theta_1,\theta_2,x_1,x_2,\omega)$$
$$=\Phi_P(\omega)\exp\left(-\frac{|\theta_1-\theta_2|}{\lambda_\theta(\omega)}\right)\exp\left(-\frac{|x_1-x_2|}{\lambda_A(\omega)}\right)\cos\left(\frac{\omega(x_1-x_2)}{V_c(\omega)}\right) \quad (43)$$

where $\lambda_\theta(\omega)$ is the pressure azimuthal correlation angle. When used to compute the auto and cross-spectral terms of the resulting random forces:

$$S_{F_yF_y}(x_1,x_2,\omega)=\frac{D^2}{4}\int_{-\pi}^{\pi}\int_{-\pi}^{\pi}S_p(\theta_1,\theta_2,x_1,x_2,\omega)\cos\theta_1\cos\theta_2\,d\theta_1 d\theta_2 \quad (44)$$

$$S_{F_zF_z}(x_1,x_2,\omega)=\frac{D^2}{4}\int_{-\pi}^{\pi}\int_{-\pi}^{\pi}S_p(\theta_1,\theta_2,x_1,x_2,\omega)\sin\theta_1\sin\theta_2\,d\theta_1 d\theta_2 \quad (45)$$

$$S_{F_yF_z}(x_1,x_2,\omega)=\frac{D^2}{4}\int_{-\pi}^{\pi}\int_{-\pi}^{\pi}S_p(\theta_1,\theta_2,x_1,x_2,\omega)\cos\theta_1\sin\theta_2\,d\theta_1 d\theta_2 \quad (46)$$
$$=S_{F_zF_y}(x_1,x_2,\omega)$$

we obtain for (44):

$$S_{F_yF_y}(x_1,x_2,\omega)=\Phi_P(\omega)\chi^2_{yy}(\lambda_\theta)\exp\left(-\frac{|x_1-x_2|}{\lambda_x(\omega)}\right)\cos\left(\frac{\omega(x_1-x_2)}{V_c(\omega)}\right) \quad (47)$$

with:

$$\chi^2_{yy}(\lambda_\theta)=\frac{D^2}{4}\int_{-\pi}^{\pi}\int_{-\pi}^{\pi}\exp\left(-\frac{|\theta_1-\theta_2|}{\lambda_\theta(\omega)}\right)\cos\theta_1\cos\theta_2\,d\theta_1 d\theta_2$$
$$=\frac{D^2}{4}\int_{-\pi}^{\pi}\left\{\begin{array}{l}\displaystyle\int_{\theta_2-\pi}^{\theta_2}\exp\left(-\frac{\theta_2-\theta_1}{\lambda_\theta(\omega)}\right)\cos\theta_1 d\theta_1\\ \displaystyle+\int_{\theta_2}^{\theta_2+\pi}\exp\left(-\frac{\theta_1-\theta_2}{\lambda_\theta(\omega)}\right)\cos\theta_1 d\theta_1\end{array}\right\}\cos\theta_2\,d\theta_2 \quad (48)$$

and similarly for the integrals (45)-(46). One thus obtain:

$$\chi^2_{yy}(\lambda_\theta)=\chi^2_{zz}(\lambda_\theta)=\frac{\pi D^2}{2}\frac{\lambda_\theta(\omega)}{1+\left[\lambda_\theta(\omega)\right]^2}\left[1+\exp\left(-\frac{\pi}{\lambda_\theta(\omega)}\right)\right] \quad (49)$$

and:

$$\chi^2_{yz}(\lambda_\theta)=\chi^2_{zy}(\lambda_\theta)=0 \quad , \quad \forall\lambda_\theta(\omega) \quad (50)$$

which shows that, for axial homogeneous turbulence, the two resulting orthogonal random forces will be uncorrelated, irrespective of any value of the azimuthal correlation $\lambda_\theta(\omega)$. Please note that a result different from (49) has been used by several authors, for instance Clinch [6] et Chen & Wambsganss [17], which in our view is erroneous. Actually, the manner used by these authors for performing the integration (44) ignores the correlation overlap which occurs in circular geometries. As a consequence, if they also computed integral (45) using their technique, different results would be obtained for $\chi_{yy}(\lambda_\theta)$ and $\chi_{zz}(\lambda_\theta)$, which is not acceptable. Solution (49) was also obtained by other authors, for instance Axisa [19].

The various coefficients are illustrated in Figure 9, as a function of the correlation angle. Notice that, because $\lambda_\theta(\omega)/\pi \ll 1$, coefficients (49) may be linearized in the range of interest and one obtains:

$$\chi^2_{yy}(\lambda_\theta)=\chi^2_{zz}(\lambda_\theta)=\frac{\pi D^2}{2}\left[\lambda_\theta(\omega)-(\lambda_\theta(\omega))^3+\cdots\right]\approx\frac{\pi D^2}{2}\lambda_\theta(\omega) \quad (51)$$

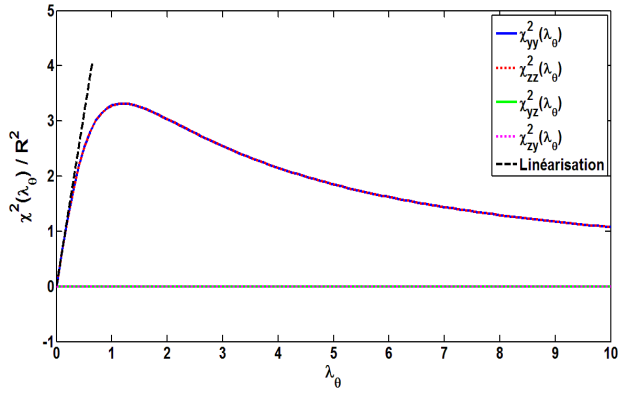

Figure 9: Change of the azimuthal spectral coefficients from the axial turbulent pressure field

Unfortunately, analysis of the turbulence from transverse flows is more difficult. Actually, flow separation generates a non-homogenous azimuthal pressure field, which renders the computation of the spectral function (44)-(46) more difficult. Nevertheless, if suitable measurements of the azimuthal correlation are available, one may also compute an objective measure of the correlation between the two orthogonal resulting forces. This issue certainly deserves to be resolved.

CONCLUSIONS

In this paper we address the practical topic of generating random force sets to simulate the turbulence excitations by transverse and axial flows in the time-domain. Computational methods previously developed by the authors have been extended to deal with the excitation by axial flows. Illustrative computations of several excitation cases were presented and the dynamical effects of turbulence convection illustrated.

Both turbulence emulation techniques presented in this paper proved adequate and reliable. They constitute a sound excitation basis, on which realistic linear and nonlinear time-domain numerical simulations of flow-excited multi-supported tubes can be achieved. Our simplified force generation method, although less physically tangible that Shinozuka's technique, is computationally much faster. Therefore we believe that both approaches are equally interesting and useful.

REFERENCES

[1] Axisa, F., Antunes, J., Villard, B. (1990) "Random excitation of heat-exchanger tubes by cross-flows". *Journal of Fluids and Structures*, Vol. 4, pp. 321-341

[2] Antunes, J., Delaune, X., Piteau, P., Borsoi, L. (2008), "A simple consistent method for the time-domain simulation of turbulence excitations applied to tube/support dynamical analysis under non-uniform flows", *9th International Conference on Flow Induced Vibrations (FIV-2008)*, 30 June-3 July 2008, Prague, Czech Republic.

[3] Antunes, J., Piteau, P., Delaune, X., Borsoi, L. (2009), "An evaluation of methods for the time-domain simulation of turbulence excitations for tube bundles subjected to non-uniform flows", *20th International Conference on Structural Mechanics in Reactor Technology (SMIRT 20)*, 9-14 August 2009, Espoo, Finland.

[4] Shinozuka, M., Yun, C., Seya, H. 1990. Stochastic methods in wind engineering. *Journal of Wind Engineering and Industrial Aerodynamics*, Vol. 36, pp. 829-843.

[5] Corcos, G. M. (1964) "The structure of the turbulent pressure field in boundary layer flow". *Journal of Fluid Mechanics*, Vol. 18, pp. 353-378.

[6] Clinch, J. M. (1969) "Measurement of the wall pressure field at the surface of a smooth-walled pipe containing turbulent water flow". *Journal of Sound and Vibration*, Vol. 9, pp. 398-419.

[7] Willmarth, W. W., Wooldridge, C. E. (1962) "Measurements of the fluctuating pressure at the wall beneath a thick turbulent boundary layer". *Journal of Fluid Mechanics*, Vol. 14, pp. 187-210.

[8] Bull, M.K. (1967) "Wall-pressure fluctuations associated with subsonic turbulent boundary layer flow". *Journal of Fluid Mechanics*, Vol. 28, pp. 719-754.

[9] Bakewell, H.P. (1968) "Turbulent wall pressure fluctuations on a body of revolution". *Journal of the Acoustical Society of America*, Vol. 43, pp. 1358-1363.

[10] Gorman, D. J. (1971) "An analytical and experimental investigation of the vibration of cylindrical reactor fuel elements in two-phase parallel flow". *Nuclear Science and Engineering*, Vol. 44, pp. 277-290.

[11] Au-Yang, M.K. (2001) "Flow-induced vibration of power and process plant components : A practical workbook". ASME Press, New York, USA.

[12] Durant, C., Robert, G., Filippi, P.J.T, Mattei, P.-O. (2000) "Vibroacoustic response of a thin cylindrical shell excited by a turbulent internal flow: Comparison between numerical prediction and experimentation". *Journal of Sound and Vibration*, Vol. 229, pp. 1115-833.

[13] Leclercq, D. J., Bohineust, X. (2002) "Investigation and modelling of the wall pressure field beneath a turbulent boundary layer at low and medium frequencies". *Journal of Sound and Vibration*, Vol. 257, pp. 477-501.

[14] Van Dyke, M. (1982) "An album of fluid motion", The Parabolic Press, Stanford, USA.

[15] Piteau, P., Delaune, X., Antunes, J., Borsoi, L. (2010), "Vibro-impact experiments and computations of a gap-supported tube subjected to single-phase fluid-elastic coupling forces", *7th International Symposium on Fluid-Structure Interactions, Flow-Sound Interactions, Flow-Induced Vibration and Noise*, 1-5 August 2010, Montreal, Canada.

[16] Inada, F., Yoneda, K., Yasuo, A., Nishihara, T. (2007) "A study on fluid excitation forces acting on a rotated square tube bundle of T/D=3.1 in cross-flow". *ASME Journal f Pressure Vessel Technology*, Vol. 129, pp. 162-168.

[17] Chen, S.S., Wambsganss, M.W. (1972) "Parallel-flow-induced vibration of fuel rods". *Nuclear Engineering and Design*, Vol. 18, pp. 253-278.

[18] Bolotin, V. V. (1984) "Random vibrations of elastic systems". Martinus Nijhoff Publishers, The Hague, The Netherlands.

[19] Axisa, F. (2001) "Modélisation des systèmes mécaniques: Tome 4 - Vibrations sous écoulements" (*in French*). Hermes, Paris, France.